

# Differences in intracellular calcium dynamics cause differences in $\alpha$ -granule secretion and phosphatidylserine expression in platelets adhering on glass and TiO<sub>2</sub>

Swati Gupta

*Biosurfaces, CIC biomaGUNE, Paseo Miramón 182, San Sebastián 20009, Spain and  
Department of Biochemistry and Molecular Biology, University of the Basque Country, 28940 Leioa, Spain*

Alessia Donati

*Institute of Functional Interfaces (IFG), Karlsruhe Institute of Technology (KIT),  
Hermann-von Helmholtz-Platz 1, 76344 Eggenstein-Leopoldshafen, Germany*

Ilya Reviakine<sup>a)</sup>

*Institute of Functional Interfaces (IFG), Karlsruhe Institute of Technology (KIT),  
Hermann-von Helmholtz-Platz 1, 76344 Eggenstein-Leopoldshafen, Germany and  
Department of Bioengineering, University of Washington, Seattle, Washington 98105*

(Received 12 February 2016; accepted 6 April 2016; published 27 April 2016)

In this study, the activation of purified human platelets due to their adhesion on glass and TiO<sub>2</sub> in the absence of extracellular calcium was investigated. Differences in  $\alpha$ -granule secretion between platelets adhering on the two surfaces were detected by examining the expression and secretion of the  $\alpha$ -granule markers P-selectin (CD62P) and  $\beta$ -thromboglobulin. Similarly, differences in the expression of phosphatidylserine (PS), and in the activation of the major integrin GPIIb/IIIa, on the surfaces of the adhering platelets, were also observed. While all of these activation markers were expressed in platelets adhering on glass, the surface markers were not expressed in platelets adhering on TiO<sub>2</sub>, and  $\beta$ -thromboglobulin secretion levels were substantially reduced. Differences in marker expression and secretion correlated with differences in the intracellular calcium dynamics. Calcium ionophore treatment triggered  $\alpha$ -granule secretion and PS expression in TiO<sub>2</sub>-adhering platelets but had no effect on the activation of GPIIb/IIIa. These results demonstrate specificity in the way surfaces of artificial materials activate platelets, link differences in the intracellular calcium dynamics observed in the platelets adhering on the two surfaces to the differences in some of the platelet responses ( $\alpha$ -granule secretion and PS expression), but also highlight the involvement of synergistic, calcium-independent pathways in platelet activation. The ability to control activation in surface-adhering platelets makes this an attractive model system for studying platelet signaling pathways and for tissue engineering applications. © 2016 American Vacuum Society. [<http://dx.doi.org/10.1116/1.4947047>]

## I. INTRODUCTION

Platelets are anuclear cell fragments circulating in blood, whose main function is to catalyze clot formation at the site of vascular injury—a mechanism for limiting traumatic blood loss called hemostasis.<sup>1,2</sup> Several well-known bleeding disorders are associated with platelet dysfunction.<sup>3,4</sup> Platelets are also known for their sinister role in pathological coagulation, or thrombosis, that leads to heart attacks and strokes.<sup>5</sup> These thrombotic complications are commonly caused by atherosclerosis that starts as an inflammation of the arterial wall, a process also mediated by the platelets.<sup>6</sup> Stents, widely used to restore blood flow in arteries occluded by atherosclerotic plaques, similarly cause thrombotic and inflammatory complications that are mediated by the platelets—as do all devices that come into contact with blood in the context of modern medical treatments.<sup>7–10</sup> Antiplatelet therapies are widely used to manage these complications.<sup>11</sup> The key step in the platelet-mediated reactions is platelet activation.

Several features distinguish activated platelets from the quiescent ones that normally circulate in blood. Activation causes platelets to change shape and increase in size. Activated platelets interact with plasma proteins, such as fibrinogen, and other cells (e.g., leukocytes),<sup>12</sup> aggregate, express phosphatidylserine (PS) on their surfaces to catalyze clot formation,<sup>13</sup> and secrete the contents of their storage granules: hemostatic mediators, growth factors, and cytokines.<sup>14</sup> Activation is triggered by agonists interacting with specific receptors.<sup>2</sup> It proceeds through a cascade of signaling pathways involving a rise in the intracellular calcium<sup>15</sup> and a number of autocatalytic loops<sup>16</sup> to the responses listed above. Examples of most important physiological agonists include thrombin, adenosine diphosphate, thromboxane, von Willebrand factor (vWF) adsorbed to collagen, and collagen itself that is present at the sites of vascular injury.<sup>2</sup> Phorbol myristoyl acetate (PMA), thrombin analogs such as thrombin receptor activating peptide (TRAP), and calcium ionophore, which directly rises intracellular calcium, are commonly used to activate platelets *in vitro*.<sup>17</sup> Sets of responses induced by different agonists and their combinations are subtly different. These differences are now thought to reflect different functional aspects of platelet responses in the

<sup>a)</sup> Author to whom correspondence should be addressed; electronic mail: [Ilya.Reviakine@kit.edu](mailto:Ilya.Reviakine@kit.edu)

context of their hemostatic, inflammatory, and other physiological and pathological roles.<sup>18</sup> Much remains to be learned about platelet signaling pathways and especially about interactions between them. In the context of unraveling interactions between signaling pathways, experiments with purified platelets adhering on artificial surfaces may become particularly useful, because of the absence of plasmatic factors that complete the activation feedback loops; this aspect has been recently reviewed in Ref. 16.

In comparison with molecular agonists, much less is known about how artificial surfaces activate platelets. The studies that have been done are mostly observational; although a few mechanistic studies have also been performed, no model has yet emerged.<sup>19–26</sup> Systematic immunolabeling of several activation markers has, to the best of our knowledge, not been undertaken yet. In this context, our recent observation of surface-specific CD62P expression in adhering platelets<sup>27</sup> represents an interesting starting point for studying the specificity of platelet–biomaterial interactions and for examining combinations of signaling pathways involved in these interactions. Here, we examine the activation of adhering platelets by immunofluorescence microscopy and enzyme-linked immunosorbent assay (ELISA), focusing on the key signaling event that accompanies activation: the intracellular calcium rise.<sup>15</sup> The results of our study add to the growing body of evidence that different materials may activate platelets in different ways, engaging specific signaling pathways and leading to the expression of particular sets of activation markers.

## II. MATERIALS AND METHODS

### A. Materials

Antibodies used in this study—PerCPCy5.5-conjugated anti-CD41a (HIP8 clone, Ms IgG<sub>1</sub>, K), APC or PE-conjugated anti-CD62P (AK-4 clone, Ms IgG<sub>1</sub>, K), PE-conjugated anti-CD63 (H5C6 clone, Ms IgG<sub>1</sub>, K), FITC-conjugated PAC1 (PAC1 clone, Ms IgM, K), and their isotype matched controls—were purchased from Becton-Dickinson (Madrid, Spain or Heidelberg, Germany).

Acid-citrate-dextrose (ACD), PMA, calcium ionophore A23187 (CaIoP), and thrombin receptor activating peptide (TRAP) were purchased from Tocris Biosciences (Oxford, UK). BAPTA-AM, calcein-AM, fluo-3-AM, and red-orange calcein-AM fluorescent dyes were purchased from Invitrogen (Madrid, Spain). All other chemicals and plasticware (safe-lock Eppendorf tubes, 15 and 50 ml falcon tubes) were purchased from Sigma (Madrid, Spain). PE or APC-conjugated Annexin A5 were purchased from Becton–Dickinson (Madrid, Spain). Coated glass vacutainer<sup>®</sup> tubes (4.5 ml) with 3.8% sodium citrate anticoagulant (0.129 M) were purchased from Becton–Dickinson. Water used in the study was purified with a Diamond UV water purification system (Branstead International, IA, USA) and is referred to as Nanopure water.

Surfaces used in this study were either bare 25 mm diameter 0.13–0.16 mm thickness (#1) microscope glass coverslips (Menzel-Gläser, Braunschweig, Germany), or the same glass coverslips coated with ~20 nm layer of TiO<sub>2</sub> by magnetron

reactive sputtering. The coating was done in a Leybold dc-magnetron Z600 sputtering unit at the Paul Scherrer Institut (Villigen, Switzerland) or in a TC 1800 UHV sputtering system (AJA International, Inc., MA) equipped with a load-lock transfer chamber at CIC biomaGUNE, according to the previously published protocols.<sup>28,29</sup> Surface chemical composition was characterized by x-ray photoelectron spectroscopy to confirm the coating quality, composition, and absence of impurities. All surfaces were cleaned by incubating in 2% sodium dodecyl sulfate for 30 min, rinsing with Nanopure water, and subjecting to the UV-ozone treatment in a cleaning chamber from Bioforce, Nanosciences (Ames, AL, USA) that was preheated for 30 min before use.

### B. Methods

#### 1. Blood collection protocol

Blood collection was organized by the Biobanco Vasco para la Investigación (Basque Biobank for Research, Galdakao, Spain) and performed with informed consent according to the appropriate legal and ethical guidelines. Study protocols were approved by the Comité de Ética de Investigaciones Clínicas (CEIC, the Clinical Investigations Ethics Committee) of the Galdakao-Usansolo hospital. Blood collection at KIT was organized by the KIT medical service. Study protocols were approved by the Ethics commission of Baden-Württemberg.

In both cases, donors were healthy volunteers without the history of exposure to medication (such as aspirin) or exposure to alcohol in the 2 weeks prior to collection. For every experiment, 10 ml of blood was collected by venipuncture with a 21-gauge needle into two 4.5 ml glass Vacutainer tubes with 3.8% sodium citrate anticoagulant and stored at 37 °C. First, 2 ml of blood was discarded during the collection to avoid contamination by residual thrombin that arises from contact phase activation.<sup>30</sup>

#### 2. Preparation of washed platelets from whole blood

All experimental procedures were carried out in a sterile laminar flow cabinet to avoid contamination. Glass- and plasticware was autoclaved before use unless it was already sterile when purchased. Platelet isolation and purification was carried out using the same protocol mentioned in our previous publications.<sup>27,31</sup> To this end, citrate-anticoagulated whole blood was transferred from the Vacutainers to 1.5 ml Eppendorf Safe-lock microcentrifuge tubes (Sigma Aldrich, Madrid). Platelet count was determined with a ABX Micros 60 hematology analyzer (Horiba ABX Diagnostics, Madrid, Spain) and was typically in the range of  $1.5–2.5 \times 10^8$  platelets per ml. Platelet-rich plasma (PrP) was prepared from whole blood by centrifugation at  $37 \times g$  for 20 min at 37 °C. PrP layers were collected into a 15 ml falcon tube and ACD (Sigma, Madrid, Spain) was added to the PrP in a ratio 1:6 by volume. PrP was incubated for 10 min at 37 °C and then centrifuged at  $700 \times g$  at 22 °C for 20 min. The pellet was resuspended in citrate buffer (100 mM NaCl, 5 mM KCl, 5 mM glucose, 1 mM MgCl<sub>2</sub>, 15 mM citrate, pH 6.5) and

centrifuged again at  $700 \times g$  at  $22^\circ\text{C}$  for 10 min. The pellet was finally suspended in the 2-[4-(2-hydroxyethyl)piperazin-1-yl]ethanesulfonic acid (HEPES) isolation buffer (145 mM NaCl, 5 mM Glucose, 1 mM  $\text{MgCl}_2$ , 10 mM HEPES, 5 mM KCl, pH 7.4). For experiments to be carried out in the presence of extracellular calcium, the pellet was resuspended in the HEPES isolation buffer containing 2 mM calcium. Platelet concentration was adjusted to  $\sim 1 \times 10^8$  cells per ml based on the count from the hematology analyzer.

### 3. Flow cytometry characterization of purified platelets

The purity, level of activation of the freshly prepared platelets, and their response to agonists (TRAP and PMA) were characterized by flow cytometry. Only samples that satisfied the following criteria were used in subsequent experiments: (1) isolated suspension consisted of only one population of cells, and 95% of it stained positive for the platelet marker CD41a. (2) The level of platelet activation, as judged by the levels of expression of CD62P, PS, and GPIIb-IIIa activation, was below 5%, while the level of expression of CD63 was below 8% (Fig. S1 in the supplementary material);<sup>32</sup> (3) expression of these markers could be induced by stimulation with TRAP or PMA. Further details can be found in our previous publications<sup>27,31</sup> and Fig. S1 in the supplementary material.

At CIC biomaGUNE, platelet isolation was performed within  $\sim 12$  h of phlebotomy. The delay was due to the stringent safety regulations requiring off-site testing of blood for infectious agents before the blood could be used for experiments. We verified that platelets isolated from fresh blood behaved in the same way as platelets isolated after 12 h of blood extraction in regards to activation with soluble agonists (Fig. S1B in the supplementary material and Ref. 27). At KIT, platelets were isolated within 30 min of phlebotomy.

### 4. Preparation of platelets loaded with fluo-3 AM and red-orange calcein AM dyes

For evaluating intracellular calcium changes in adhering platelets, PrP was incubated with fluo-3 AM ( $10 \mu\text{M}$ ) and red-orange calcein AM ( $5 \mu\text{g/ml}$ ) for 40 min at  $37^\circ\text{C}$  before platelets were isolated from it. The rest of the platelet isolation, purification, and characterization procedure remained as described above.

### 5. Platelet adhesion and activation studies on glass and $\text{TiO}_2$ surfaces

All adhesion experiments were performed at  $37^\circ\text{C}$ . Freshly cleaned surfaces were mounted in home-made Teflon chambers using Picodent Twinsil 22 addition-curing duplicating silicone (Kedon S.L., Málaga, Spain) as an adhesive, or in metal holders housing Teflon spacers over the glass coverslips. The Picodent adhesive did not spread to the portion of surface that came in contact with the platelets, and no difference in the results obtained with the two types of sample cells could be discerned.  $250 \mu\text{l}$  of the calcium free or calcium-containing HEPES buffer (depending on the experiment) were added to the Teflon cells immediately after

the glue had set ( $\sim 2$  minutes after application) to reduce as much as possible the chances of contaminating the surface.  $250 \mu\text{l}$  of the washed platelets in the same buffer were then added to the buffer and incubated either for 10 mins or for 3 hrs.

After the incubation, the samples were washed by adding and withdrawing  $250 \mu\text{l}$  of the buffer  $20\times$  to remove any nonadherent platelets. Care was taken not to touch the surface with the pipette tip, not to introduce bubbles, and not to dry the sample out.

Washed samples were costained with  $5 \mu\text{l}$  of PerCPCy5.5 anti-CD41a antibody and one of the reagents specific for the other platelet activation markers: activated GPIIb/IIIa, or PS. FITC-conjugated PAC1 antibody was used for the former, PE-conjugated A5 was used for the latter. After the addition of antibodies, the samples were incubated for 30 min before being analyzed by confocal microscopy.

For the experiments involving stimulation of surface-adhered platelets with agonists, the above-described steps were followed by the addition of TRAP, PMA, or  $\text{CaIoP}$ , to the sample cell. In other experiments calcium ionophore along with 2 mM calcium was added to the adhered platelets. Samples were incubated with agonists for 30 min, followed by analysis with confocal microscopy.

### 6. Confocal microscopy

Fluorescence and transmission images of adhering platelets were obtained using a Zeiss LSM 510 confocal laser scanning microscope equipped with a plan-Apochromat  $63\times/1.40$  NA oil immersion objective (for the analysis of marker expression on the adhering platelets, Figs. 1(a), 3, 4, and S6 in the supplementary material) or  $40\times$  EC-plan-Neofluar  $1.30$  NA oil immersion objective (for the real-time intracellular calcium level measurements, Fig. 2 and movies S4 and S5 in the supplementary material), or with a Zeiss epifluorescence microscope equipped with a Colibri illumination system (Figs. S3 and S7 in the supplementary material). All experiments were carried out in a temperature controlled stage at  $37^\circ\text{C}$ .

*a. Analysis of marker expression on the adhering platelets.* PerCP Cy5.5, FITC, and PE fluorescence was excited with the 488 nm line of the Ar laser and emission was measured at 695, 519, and 578 nm, respectively.

*b. Real-time analysis of platelet adhesion and intracellular calcium level measurements.* For the analysis of intracellular calcium, the above procedure was modified. Assembled and buffer-filled Teflon cells were first mounted on the confocal microscope stage. The objective was focused on the sample surface. Imaging was started, and then  $20 \mu\text{l}$  of the labeled platelets were added to the cell. In this manner, their adsorption to the surface could be continuously monitored.

Fluorescence of the fluo-3 and red-orange calcein dyes was measured simultaneously using 505/530 nm excitation/emission 570/590 nm excitation/emission, respectively. With

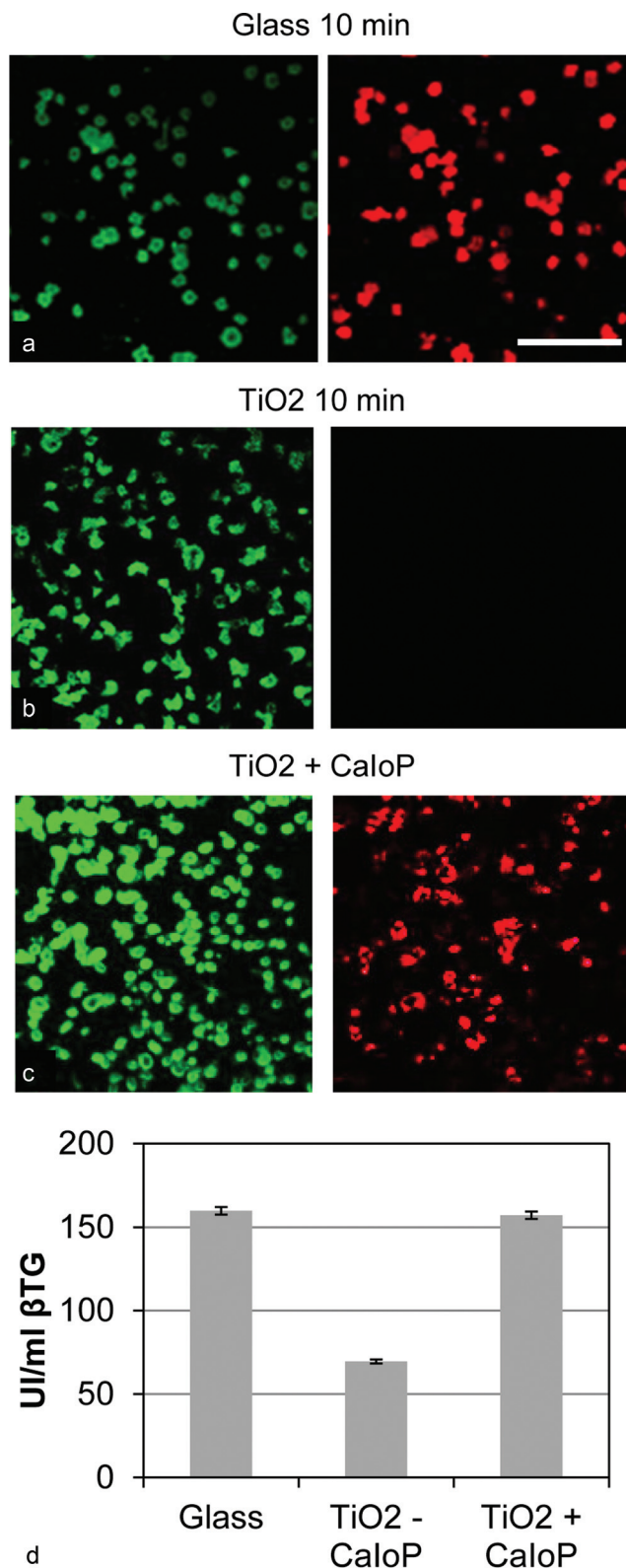


Fig. 1. Controlling  $\alpha$ -granule secretion in adhering platelets. Immunofluorescence staining reveals CD62P expression patterns on platelets adhering on glass (a) and TiO<sub>2</sub> (b) in the absence of extracellular calcium. Purified platelets were allowed to adhere to the two substrates for 10 min, rinsed and stained with aCD41a (green) and aCD62P (red) antibodies. Treatment with CaloP in a calcium-containing buffer (c) triggered CD62P expression. Scale bar, shown in (a), is 50  $\mu$ m. The results of  $\beta$ -thromboglobulin analysis by ELISA are shown in (d). The secretion of this factor is high in platelets adhering on glass, low in platelets adhering on TiO<sub>2</sub> in the absence of extracellular calcium, but increases after their treatment with the calcium ionophore in a calcium-containing buffer. Averages from five independent experiments performed with blood obtained from different donors are shown; error bars represent standard deviations. Note that the data on TiO<sub>2</sub> were obtained on the same samples in each of the five experiments; what is shown, therefore, is an increase in the  $\beta$ -thromboglobulin level as a result of the ionophore treatment.

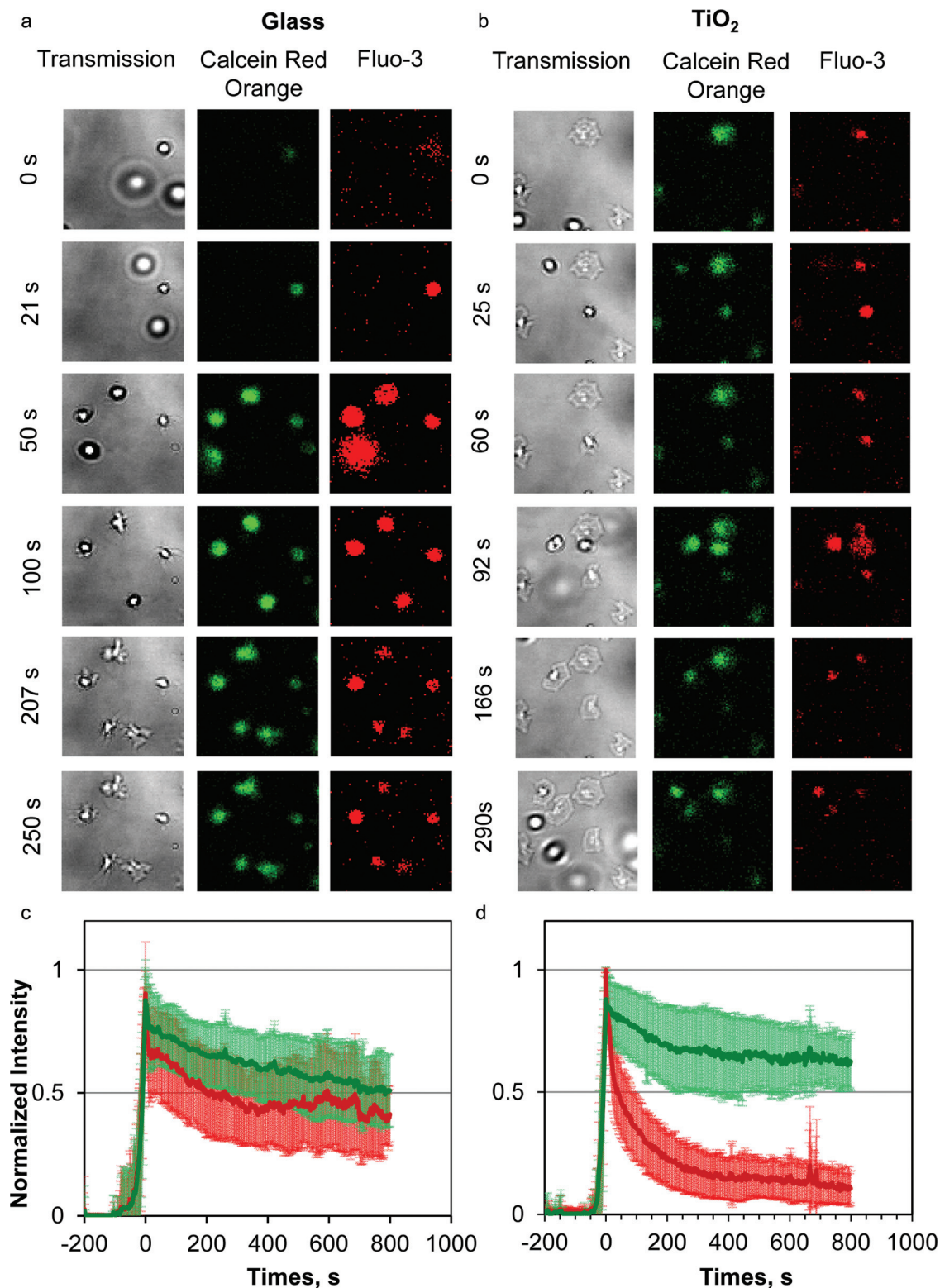


FIG. 2. Following the intracellular calcium dynamics in the adhering platelets. Transmission images (left), calcein red orange (middle, green), and the calcium-sensitive fluo-3 (right, red) fluorescence images of platelets adhering onto glass (a) and TiO<sub>2</sub> (b). Fluo-3 is nonfluorescent without calcium present (in resting platelets) but its fluorescence increases at least 40 times upon calcium binding (in activated platelets). Calcein red orange fluorescence is independent of intracellular calcium concentration. It is used as a reporter dye to follow the evolution of platelets at the surface. The images are  $34 \times 34 \mu\text{m}$ . Fluorescence intensity of individual platelets, such as those visible in (a) and (b), was analyzed as described in Sec. II and plotted as a function of time, normalized to the maximal intensity for each dye on each surface. The normalization factors were found to correlate between the two channels (calcein red orange and fluo-3), indicating that they were not related to the heterogeneity in the intracellular calcium dynamics between different platelets. Individual normalized traces were then averaged. The plots of normalized and averaged traces containing data from 34 and 44 platelets are shown in (c) and (d) for glass and TiO<sub>2</sub>, respectively. Error bars, visible in a lighter color above and below the lines representing the plotted data, are standard deviations.

these optical conditions, there was no interference between the two dyes. The process of platelet sedimentation and adhesion was recorded at a rate of 1.2 images/s.

### 7. Image analysis

To generate the plots shown in Fig. 2, images were analyzed with the IMAGEJ or FIJI software.<sup>33,34</sup> The analysis proceeded as follows. Contours of individual adhering platelets were manually drawn around the platelets in the transmission images. Median fluorescence intensities within these contours were then obtained for each frame within each channel using the measurement function of the IMAGEJ software. Background intensities were obtained in a similar way for each channel but in the areas of the images which did not contain any platelets. Background intensities were subtracted from the intensities within the cells. The background-subtracted intensities were then normalized to the maximal value for each dye. The time-sequences of the normalized background-subtracted intensities of individual cells were aligned such that the rise in the intensity to its maximal value apparent in Fig. 2 coincided for all cells. Finally, for each of the two conditions (glass versus TiO<sub>2</sub>), the normalized intensities were averaged. The resulting normalized, averaged data are plotted in Figs. 2(c) and 2(d), for glass and TiO<sub>2</sub>, respectively.

### 8. Analysis of $\beta$ -thromboglobulin secretion by the adherent platelets by ELISA

Sample preparation followed the same steps as for fluorescence microscopy above. After the platelets were allowed to adhere to the surface for 10 min, the buffer was collected, centrifuged to pellet the nonadherent platelets, and flash-frozen in liquid nitrogen. For evaluating the effect of CaIoP on the platelets adhering on TiO<sub>2</sub>, the buffer over the adhering platelets was then replaced with a calcium-containing buffer containing CaIoP at a concentration of 5  $\mu$ M. After a 30 min incubation with CaIoP, the buffer was collected, centrifuged, and the supernatant—flash-frozen.  $\beta$ -thromboglobulin ELISA kit (Stago, Germany) was used to determine  $\beta$ -thromboglobulin concentration in the samples according to manufacturer's specifications.

## III. RESULTS

### A. Platelet isolation and characterization

In our study, we used platelets purified by centrifugation from citrate-anticoagulated blood according to the procedure we described previously,<sup>27,31,35</sup> further details are provided in Sec. II. Prior to the adhesion experiments, the activation levels of the purified platelets and their response to agonists (TRAP and PMA) were ascertained by flow cytometry. This was done immediately after purification. The acceptable fraction of isolated platelets expressing standard activation markers was below 5% for CD62P, PS, and activated GPIIb/IIIa, and below 8% for CD63. In agonist-treated platelets (TRAP or PMA), this fraction was 80%–90% for CD62P, CD63, and activated GPIIb/IIIa, and 5%–12% for PS.<sup>31,35</sup>

For further details, see Fig. S1A in the supplementary material and our previous publications.<sup>27,31,35</sup>

During this study, we took advantage of an opportunity to investigate the effect of whole blood storage prior to platelet purification on platelet activation. In particular, results of experiments with platelets purified immediately after phlebotomy and 12–24 h after phlebotomy were compared with each other. In the latter case, citrate-anticoagulated blood was stored at room temperature without agitation. Figure S1B shows the results of this comparison for platelets in solution. Platelets purified 24 h after phlebotomy expressed similar amounts of the four activation markers as those purified within 1–2 h after phlebotomy. The results of the surface adhesion experiments were also not affected by the delay; they are presented and discussed below.

### B. Calcium ionophore treatment triggers $\alpha$ -granule secretion in platelets adhering on TiO<sub>2</sub>

We reported previously that purified platelets adhering on TiO<sub>2</sub> in the absence of extracellular calcium did not express the  $\alpha$ -granule marker CD62P, while platelets adhering on glass under the same conditions did [Figs. 1(a) and 1(b)].<sup>27</sup> Platelets adhering on both surfaces expressed dense granule marker CD63 (Ref. 36) (Fig. S2 in supplementary material and Ref. 27). Exposing adhering platelets to extracellular calcium or agonists such as TRAP after adhesion did not have an effect on CD62P expression.<sup>27</sup> Treating the TiO<sub>2</sub>-adherent platelets with CaIoP in the presence of 2 mM Ca triggered CD62P expression [Fig. 1(c)]. Identical results were obtained with freshly purified platelets (Fig. S3 in supplementary material) as with platelets purified from blood stored for 12 h at room temperature without agitation (Fig. 1).

To further confirm our assertion that  $\alpha$ -granule secretion differed in the platelets adhering to the two surfaces (TiO<sub>2</sub> and glass), and before and after CaIoP treatment on TiO<sub>2</sub>, we measured the levels of  $\beta$ -thromboglobulin released by the adhering platelets. The results are shown in Fig. 1(d). The level of  $\beta$ -thromboglobulin was high in platelets adhering on glass, significantly lower in platelets adhering on TiO<sub>2</sub>, but increased after the platelets adhering on TiO<sub>2</sub> were treated with CaIoP [Fig. 1(e)].  $\beta$ -thromboglobulin levels therefore correlated with the pattern of CD62P expression [Figs. 1(a)–1(d)].

### C. Intracellular calcium dynamics is different in platelets adhering on glass and on TiO<sub>2</sub>

Having established that calcium ionophore treatment triggers the expression and secretion of the  $\alpha$ -granule markers CD62P and  $\beta$ -thromboglobulin in platelets adhering on TiO<sub>2</sub>, we searched for the differences in the intracellular calcium dynamics in platelets adhering on the two surfaces (glass and TiO<sub>2</sub>) using a Ca-sensitive fluo-3-AM dye. It is a membrane-permeable molecule that is hydrolyzed by intracellular esterases leaving the membrane-impermeable fluo-3 dye the emission intensity of which is proportional to the cytoplasmic calcium concentration.<sup>37</sup> In the case of platelets adhering to the surface, the evolution of the platelets in the field of view

affects signal intensity. To account for these contributions to the fluorescence intensity changes as the platelets approached and adhered to the surface, we used another cell membrane permeable dye, red orange calcein AM,<sup>38</sup> which is not sensitive to calcium concentration. The results of the experiments are shown in Fig. 2 and movies S4 and S5 in the supplementary material, where the Ca-sensitive dye is represented with a red color, while the control—with a green color.

On both surfaces, platelets adhere and spread [Figs. 2(a) and 2(b)]. On both surfaces, the location of their first contact was not necessarily the same as that of the final attachment [Figs. 2(a) and 2(b)], indicating some sort of a “negotiation” between the platelet and the surface, possibly involving secretion of adhesive proteins or a search for locations on which they are already present due to the action of previously adhered platelets. These aspects remain to be investigated.

Normalized fluorescence intensities for the two dyes are plotted as a function of time for platelets adhering on glass and TiO<sub>2</sub> in Figs. 2(c) and 2(d), respectively. Several features are apparent in the averaged data. First of all, there is an increase in the fluorescence intensity of both dyes on both surfaces when platelets attach and begin to spread (this is set as time zero). This implies that part of the increase in the intensity of the Ca-sensitive dye comes not from the changes in the intracellular calcium concentration, but from the platelet rearrangements during attachment and spreading. For this reason, we decided not to convert the intensity changes into the changes in the calcium concentration. It would have been advantageous to use the Fura-2 dye instead, with which a ratio of intensities at two wavelengths is used to quantify the level of calcium; unfortunately, this option was not compatible with our equipment.

Subsequent to the rise, differences between platelets adhering on glass and on TiO<sub>2</sub> become apparent. While in platelets adhering on glass, the intensity of the calcium sensitive dye remains high, it drops significantly in the platelets adhering on TiO<sub>2</sub>.

The differences in the intensity of the Ca-sensitive dye between the two surfaces [Figs. 2(c) and 2(d)] are not reflected in the intensity of the control dye. These differences therefore reflect actual changes in the intracellular calcium concentrations rather than dye leakage, volume changes, or other platelet rearrangements. (The integrity of the adhering platelet membranes was also verified in separate experiments as shown in Fig. S6 in the supplementary material.) This interpretation is supported by comparing our results with numerous measurements of intracellular calcium dynamics available in the literature: both types of responses we observe in Fig. 2 are consistent with what has been reported for agonist-treated platelets, while the time-scale of the calcium rise and fall on TiO<sub>2</sub> is only slightly longer than that observed in platelets stimulated with thrombin in solution (~3 min).<sup>39,40</sup>

#### D. Expression of PS and aGPIIb/IIIa in surface-adhering platelets with and without the CaloP treatment

Two other important platelet activation markers are PS and the active form of GPIIb/IIIa. PS is a phospholipid that

becomes exposed on the surface of activated platelets, where it catalyzes the assembly of coagulation pathway intermediates.<sup>13,41–44</sup> GPIIb/IIIa (integrin  $\alpha$ IIB $\beta$ 3) is responsible for platelet adhesion and aggregation and is a key signaling molecule.<sup>2</sup> In platelets adhering on glass, the expression of both markers was observed in the adhering platelets [Figs. 3(a) and 4(a)] On the contrary, in platelets adhering on TiO<sub>2</sub> in the absence of calcium, neither marker was expressed [Figs. 3(b) and 4(b)]. Staining for PS was done with annexin A5, while staining for aGPIIb/IIIa was done with the PAC1 antibody. Both sets of interactions depend on calcium,<sup>45,46</sup> and therefore in both cases, calcium was added to the platelets after they were allowed to adhere in the Ca-free media.

Treatment of the TiO<sub>2</sub>-adhering platelets with CaloP + calcium triggered the expression of PS on their surfaces [Fig. 3(c)] much as it did  $\alpha$ -granule secretion (Fig. 1). On the

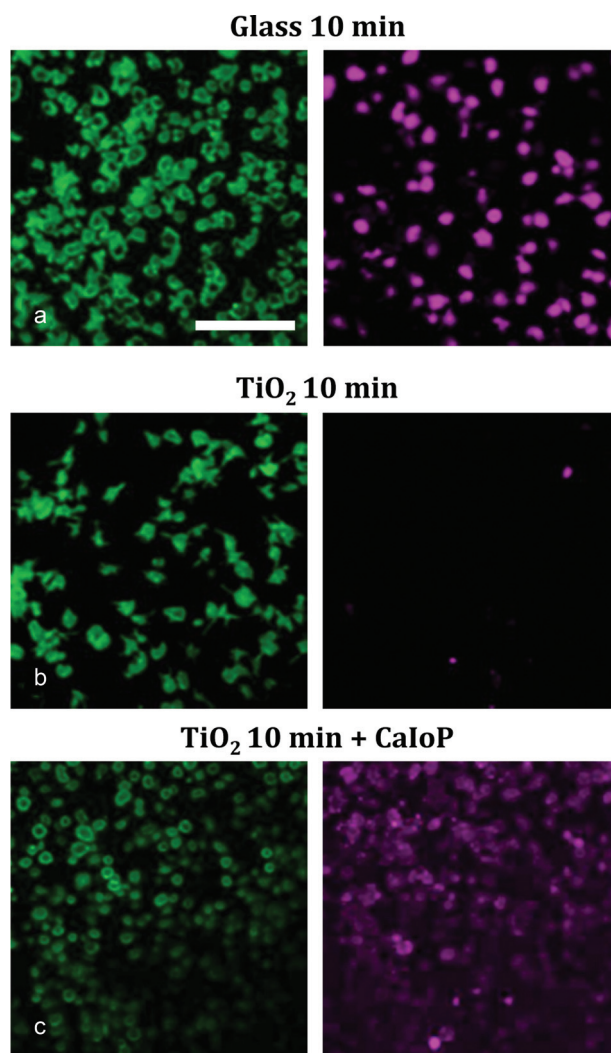


FIG. 3. Expression of PS in adhering platelets. Purified platelets were allowed to adhere to the surfaces of glass or TiO<sub>2</sub> in a calcium-free buffer for 10 min, rinsed with the calcium-containing buffer, and stained with CD41a (green) and annexin A5 (purple). PS is expressed on platelets adhering onto glass (a) but not TiO<sub>2</sub> (b) treatment of the TiO<sub>2</sub>-adhering platelets with CaloP triggers PS expression (c). Scale bar in (a) is 50  $\mu$ m.

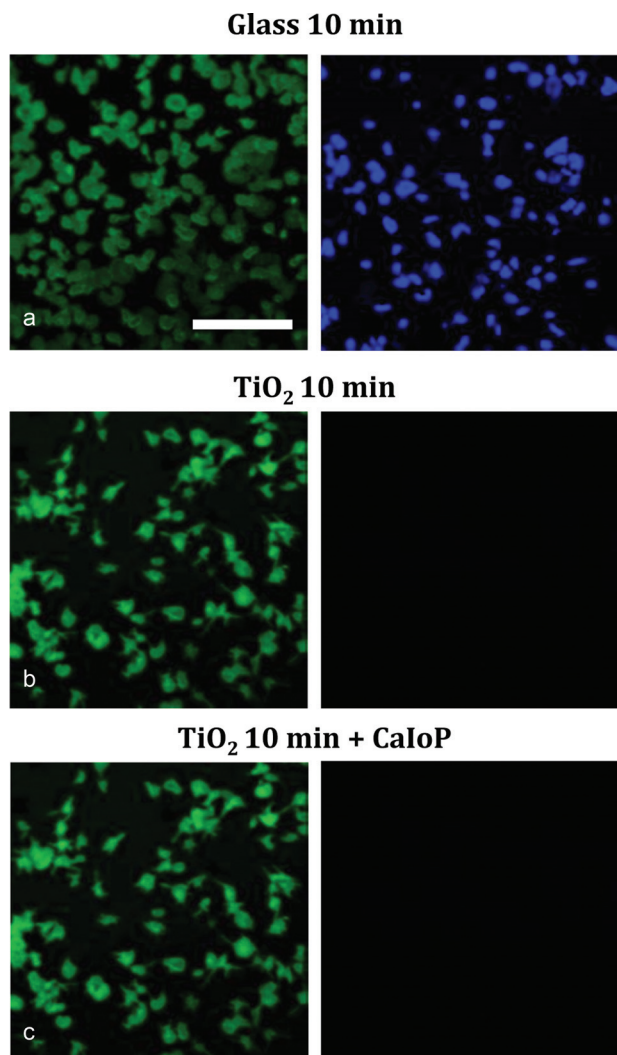


Fig. 4. Expression of aGPIIb/IIIa in adhering platelets. Purified platelets were allowed to adhere to the surfaces of glass (a) or TiO<sub>2</sub> [(b) and (c)] in a calcium-free buffer for 10 min, rinsed with the calcium-containing buffer, and stained with CD41a (green) and PAC1 antibody against the activated form of GPIIb/IIIa (blue). No GPIIb/IIIa activation is evident in TiO<sub>2</sub>-adhering platelets, before (B) or after (C) CaloP treatment. Scale bar in (a) is 50  $\mu$ m.

contrary, no effect on the expression of aGPIIb/IIIa was observed [Fig. 4(c)].

Once again, no effect of blood storage prior to platelet purification on either of these results could be discerned (cf. the results shown in Figs. 3, 4, and S7 in supplementary material).

#### IV. DISCUSSION

First, we report differences in the patterns of activation marker expression on platelets adhering on glass versus TiO<sub>2</sub> in the absence of extracellular calcium. On glass, CD63 (dense granule marker), CD62P ( $\alpha$ -granule marker), and PS are expressed, while GPIIb/IIIa is activated. On TiO<sub>2</sub>, only CD63 is expressed. Such differences have previously been noted by others. For example, Haycox and Ratner reported a passivating layer of platelets that did not express

the activated form of GPIIb/IIIa on polyethylene, in contrast to other surfaces.<sup>19</sup> Significantly, their observations were made in whole blood under flow. It is noteworthy that their passivating platelets are functionally similar to the ones we observe on TiO<sub>2</sub> in the sense that they also do not express activated GPIIb/IIIa. The discussion of platelet passivation of biomaterials in the context of cardiopulmonary bypass can also be found in Ref. 47. Similarly, Kang *et al.* observed  $\alpha$ -granule secretion in platelets adhering on peptide-coated glass surfaces only at a specific range of water contact angles (surface hydrophobicities); on the contrary, dense granule secretion did not depend on the surface properties but only on the number of the adhering platelets.<sup>26</sup> We had previously noted a parallel with our results in that the dense marker CD63 is expressed in platelets adhering both on glass and on TiO<sub>2</sub>, while  $\alpha$ -granule secretion is observed on glass but not on TiO<sub>2</sub> (Ref. 27 and this study). Broberg *et al.* noted the particular importance of surface-adsorbed von Willebrand factor for the expression of CD62P in adhering platelets.<sup>22,48</sup>

Second, we show that differences in the intracellular calcium dynamics are responsible for the difference in  $\alpha$ -granule secretion and PS expression in platelets adhering on glass and TiO<sub>2</sub>. We show this in two ways. On the one hand, the differences in the intracellular calcium dynamics correlated with the differences in the  $\alpha$ -granule secretion and PS expression between platelets adhering on the two surfaces. On the other hand, treating TiO<sub>2</sub>-adhering platelets with CaloP triggered  $\alpha$ -granule secretion and PS expression, establishing causation.

Intracellular calcium rise is a key signaling step that is essential for platelet activation.<sup>15,49</sup> It is located downstream of the agonist receptors and, through a network of calcium sensor proteins, mediates activation responses such as spreading, GPIIb/IIIa activation and adhesion, granule secretion, thromboxane production, and PS expression.<sup>49</sup> Different responses have different internal calcium concentration thresholds while agonists can be distinguished by the dynamics of the calcium rise.<sup>39,50–52</sup> Therefore, observing a causal link between a particular surface, expression of platelet activation markers, and intracellular calcium dynamics in adhering platelets, implies specificity in the way artificial surfaces activate platelets.

Others have studied intracellular calcium dynamics in adhering platelets.<sup>53–58</sup> Ikeda *et al.* observed a sustained increase in the intracellular calcium level on poly(lysine)- and fibrinogen coated surfaces but not on glass, where a peak followed by a drop to a level somewhat above the baseline was reported.<sup>54</sup> Those authors used the same calcium dye as we did, but did not control for the changes in the intensity due to platelet evolution with another dye. A rather heterogeneous response was observed by Jen *et al.* in platelets adhering on fibrinogen under flow.<sup>55</sup> Waples *et al.* reported a calcium rise that then decreased but to a level significantly above baseline in platelets adhering on glass.<sup>57</sup> They also noted calcium transients during platelet–platelet encounters—something we also observe (supplementary material movies S4 and S5). Particularly noteworthy is the

work of Okano *et al.*, who noted material-specific differences in the intracellular calcium dynamics on two pure polymers and their copolymers that were attributed to surface hydrophobicity and nanostructure; they also reported differences in the intracellular calcium dynamics induced by agonist treatment in platelets adhering on different materials.<sup>53</sup> However, in none of these studies was calcium dynamics in the adhering platelets correlated with platelet activation events.

Third, we show that differences in the intracellular calcium dynamics are not the only factor responsible for the differences in the activation of the GPIIb/IIIa integrin receptor complexes, because CaIoP treatment did not trigger GPIIb/IIIa activation in TiO<sub>2</sub>-adhering platelets. Generally, this observation fits with the idea of specificity articulated above because calcium rise is necessary but not sufficient for some of the platelet activation responses, serving instead a gating function between synergistic pathways.<sup>50</sup> Unfortunately, the interplay between different signaling pathways in platelets is not sufficiently well-understood to draw a specific conclusion, although it is thought that PS expression and GPIIb/IIIa activation are triggered through different pathways.<sup>49</sup>

Our study contributes to the accumulating body of evidence that different surfaces activate platelets in different ways, much like different agonists do. The notion of specific activation of platelets by surfaces of artificial materials has consequences for the understanding of how existing implants function as well as for the design of the new implants that actively interact with their biological environment by eliciting specific responses. Here, the future is behind structures that are able to interact with the body and integrate into the signaling pathways of the wound healing cascade.<sup>59</sup> There are also possible implications for tissue engineering applications, where stem cell differentiation may be controlled through platelets adhering to material surfaces. Platelet relatives are already being used to control stem cell fate.<sup>60–63</sup>

The origin of the platelet–biomaterial interaction specificity remains unclear. The search for it should focus on the compositions of the surface-adsorbed protein films and on the conformations of the adsorbed proteins in these films. Indeed, upon adsorption, proteins that normally do not interact with platelets undergo conformational changes rendering them platelet-adhesive.<sup>25,64–66</sup> This occurs in a manner similar to the flow-induced changes in vWF conformation that expose cryptic platelet-activating motifs, effectively turning this protein into a platelet agonist.<sup>67–69</sup> Protein film compositions have also been shown to differ between different surfaces, e.g., in studies with model solutions.<sup>70</sup> To date, the most comprehensive review in this area is that of the work done with nanoparticles.<sup>71</sup> Except for the work of Broberg mentioned above,<sup>22,48</sup> a relationship between the properties of the adsorbed protein films and platelet activation has not yet been established, although much work has been done in relating the conformational changes in the adsorbed protein films and platelet adhesion.<sup>25,65,66</sup> One of the relevant findings of these studies is that adsorption-induced conformational changes become apparent faster, when proteins adsorb

at low concentrations, than when they adsorb at high concentrations. The difference in the timescales can be significant: minutes at low concentrations versus months at high concentrations.<sup>25,65,66</sup> In this context, the studies with purified platelets may reveal long-term aging phenomena, because they are conducted at protein concentrations that are significantly lower compared to those found in plasma.

Finally, we show that storage of whole blood prior to platelet purification does not have an effect on the phenomena we investigated in this study. Indeed, effects of whole blood storage, as opposed to the storage of purified platelets or PrP, have been discussed previously by other authors.<sup>72,73</sup> While there are well-recognized effects of blood storage on platelet function,<sup>74</sup> it appears that these effects do not encompass all of their functions.

## V. CONCLUSIONS

The most important conclusion of our study is that platelet activation by surfaces may be specific, occurring through distinct sets of signaling pathways for different surfaces. We reach this conclusion based on the observation of differences in  $\alpha$ -granule secretion, PS expression, and GPIIb/IIIa activation in platelets adhering on glass and TiO<sub>2</sub> in the absence of extracellular calcium, differences in the intracellular calcium dynamics between platelets adhering on these two surfaces, the ability to trigger  $\alpha$ -granule secretion and PS expression in TiO<sub>2</sub>-adhering platelets using calcium ionophore, and lack of GPIIb/IIIa activation upon ionophore treatment.

## ACKNOWLEDGMENTS

The authors would like to acknowledge funding from the Department of Industry of the Basque Government (Program ETORTEK) and from the Spanish Ministry of Science and Innovation (MICINN, Ref. CTQ2009-11245) to I.R.; Luis Yate and Danijela Gregurec (CIC biomaGUNE, Spain) for help with the preparation and characterization of TiO<sub>2</sub>-coated glass slides; Laura Saa and Valeri Pavlov for allowing us to use their centrifuge and Nanodrop equipment; Jose Manuel Cardenas Diaz De España, Roberto Bilbao Urquiola, Amaia del Villar Álvarez, and Clara Rodriguez Aierbe (Basque Biobank for Research, Galdakao, Spain); Mari Carmen Pozo and Mari Mar Lertxundi (Basque Biobank for Research, San Sebastian, Spain) for organizing the blood collection and testing. Blood collection and testing at KIT was organized by the KIT medical service, MED, with the help of med. Volker List and Ingrid Schaefer. Financial support of the Biointerfaces in Technology and Medicine (BIF-TM) Program of the Helmholtz Association at the Karlsruhe Institute of Technology (KIT) is also gratefully acknowledged. The authors declare no competing financial interests. S.G. and A.D. performed experiments. I.R. and S.G. designed the study. S.G., A.D., and I.R. analyzed the data. I.R. wrote the manuscript.

<sup>1</sup>B. S. Coller, *J. Thromb. Haemostasis* **9**, 374 (2011).

<sup>2</sup>A. D. Michelson, *Platelets*, 3rd ed. (Academic, London, 2012).

<sup>3</sup>A. D. Michelson, *Platelets*, edited by A. D. Michelson (Academic, London, 2012), pp. 813–818.

- <sup>4</sup>B. S. Coller, *Platelets*, edited by A. D. Michelson (Academic, London, 2012), pp. xix–xliv.
- <sup>5</sup>M. Leslie, *Science* **328**, 562 (2010).
- <sup>6</sup>Z. M. Ruggeri, *Nat. Med.* **8**, 1227 (2002).
- <sup>7</sup>B. D. Ratner, *Biomaterials* **28**, 5144 (2007).
- <sup>8</sup>M. B. Gorbet and M. V. Sefton, *Biomaterials* **25**, 5681 (2004).
- <sup>9</sup>W. van Oeveren, *Scientifica* **2013**, 392584 (2013).
- <sup>10</sup>F. Jung, S. Braune, and A. Lendlein, *Clin. Hemorheol. Microcirc.* **53**, 97 (2013).
- <sup>11</sup>S. P. Jackson and S. M. Schoenwaelder, *Nat. Rev. Drug Discovery* **2**, 775 (2003).
- <sup>12</sup>J. M. van Gils, J. J. Zwaginga, and P. L. Hordijk, *J. leukocyte Biol.* **85**, 195 (2009).
- <sup>13</sup>D. M. Monroe, M. Hoffman, and H. R. Roberts, *Arterioscler., Thromb., Vasc. Biol.* **22**, 1381 (2002).
- <sup>14</sup>A. T. Nurden, *Thromb. Haemostasis* **105**, S13 (2011).
- <sup>15</sup>D. Varga-Szabo, A. Braun, and B. Nieswandt, *J. Thromb. Haemostasis* **7**, 1057 (2009).
- <sup>16</sup>I. Reviakine, *Clin. Hemorheol. Microcirc.* **60**, 133 (2015).
- <sup>17</sup>A. Michelson and S. J. Shattil, *Platelets: A Practical Approach*, edited by S. P. Watson and K. S. Authi (Oxford University, New York, 1996).
- <sup>18</sup>J. W. Heemskerk, N. J. Mattheij, and J. M. Cosemans, *J. Thromb. Haemostasis* **11**, 2 (2013).
- <sup>19</sup>C. L. Haycox and B. D. Ratner, *J. Biomed. Mater. Res.* **27**, 1181 (1993).
- <sup>20</sup>M. Broberg, C. Eriksson, and H. Nygren, *J. Lab. Clin. Med.* **139**, 163 (2002).
- <sup>21</sup>J. Y. Park, C. H. Gemmell, and J. E. Davies, *Biomaterials* **22**, 2671 (2001).
- <sup>22</sup>M. Broberg and H. Nygren, *Biomaterials* **22**, 2403 (2001).
- <sup>23</sup>S. Kanagaraja, I. Lundstrom, H. Nygren, and P. Tengvall, *Biomaterials* **17**, 2225 (1996).
- <sup>24</sup>S. L. Goodman, S. L. Cooper, and R. M. Albrecht, *J. Biomed. Mater. Res.* **27**, 683 (1993).
- <sup>25</sup>B. Sivaraman and R. A. Latour, *Biomaterials* **31**, 832 (2012).
- <sup>26</sup>I. K. Kang, Y. Ito, M. Sisido, and Y. Imanishi, *J. Biomed. Mater. Res.* **22**, 595 (1988).
- <sup>27</sup>S. Gupta and I. Reviakine, *Biointerphases* **7**, 28 (2012).
- <sup>28</sup>R. Kurrat, M. Textor, J. J. Ramsden, P. Boni, and N. D. Spencer, *Rev. Sci. Instrum.* **68**, 2172 (1997).
- <sup>29</sup>L. Zhu, D. Gregurec, and I. Reviakine, *Langmuir* **29**, 15283 (2013).
- <sup>30</sup>S. P. Watson, *Platelets: A Practical Approach* (Oxford University, New York, 1996).
- <sup>31</sup>S. Gupta and I. Reviakine, *Biochim. Biophys. Acta* **1840**, 3423 (2014).
- <sup>32</sup>See supplementary material at <http://dx.doi.org/10.1116/1.4947047> for additional information related to the characterization of platelets in solution, adhering platelets, and movies summarizing the dynamics of intracellular calcium.
- <sup>33</sup>C. A. Schneider, W. S. Rasband, and K. W. Eliceiri, *Nat. Methods* **9**, 671 (2012).
- <sup>34</sup>J. Schindelin *et al.*, *Nat. Methods* **9**, 676 (2012).
- <sup>35</sup>S. Gupta, Ph.D. thesis, University of the Basque Country, 2014.
- <sup>36</sup>M. Nishibori, B. Cham, A. McNicol, A. Shalev, N. Jain, and J. M. Gerrard, *J. Clin. Invest.* **91**, 1775 (1993).
- <sup>37</sup>J. E. Merritt, S. A. McCarthy, M. P. Davies, and K. E. Moores, *Biochem. J.* **269**, 513 (1990).
- <sup>38</sup>C. Dubois, L. Panicot-Dubois, J. F. Gainor, B. C. Furie, and B. Furie, *J. Clin. Invest.* **117**, 953 (2007).
- <sup>39</sup>A. Juska, *Biochem. Biophys. Res. Commun.* **412**, 537 (2011).
- <sup>40</sup>B. Brune and V. Ullrich, *J. Biol. Chem.* **266**, 19232 (1991).
- <sup>41</sup>J. E. Vance and G. Tasseva, *Biochim. Biophys. Acta* **1831**, 543 (2013).
- <sup>42</sup>K. Balasubramanian and A. J. Schroit, *Annu. Rev. Physiol.* **65**, 701 (2003).
- <sup>43</sup>R. F. Zwaal, P. Comfurius, and E. M. Bevers, *Biochim. Biophys. Acta* **1376**, 433 (1998).
- <sup>44</sup>P. L. A. Giesen, G. M. Willems, and W. T. Hermens, *J. Biol. Chem.* **266**, 1379 (1991).
- <sup>45</sup>S. J. Shattil, J. A. Hoxie, M. Cunningham, and L. F. Brass, *J. Biol. Chem.* **260**, 11107 (1985).
- <sup>46</sup>P. Meers, *Annexins: Molecular Structure to Cellular Function*, edited by B. A. Seaton (1996), pp. 97–119.
- <sup>47</sup>B. R. Smith and H. M. Rinder, *Platelets*, edited by A. D. Michelson (Academic, London, 2012), pp. 1075–1096.
- <sup>48</sup>M. Broberg and H. Nygren, *Colloids Surf. B: Biointerfaces* **11**, 67 (1998).
- <sup>49</sup>W. Bergmeier and L. Stefanini, *J. Thromb. Haemostasis* **7**, 187 (2009).
- <sup>50</sup>T. J. Rink, S. W. Smith, and R. Y. Tsien, *FEBS Lett.* **148**, 21 (1982).
- <sup>51</sup>S. Tadokoro, T. Nakazawa, T. Kamae, K. Kiyomizu, H. Kashiwagi, S. Honda, Y. Kanakura, and Y. Tomiyama, *Blood* **117**, 250 (2011).
- <sup>52</sup>T. J. Rink, *Experientia* **44**, 97 (1988).
- <sup>53</sup>T. Okano, K. Suzuki, N. Yui, Y. Sakurai, and S. Nakahama, *J. Biomed. Mater. Res.* **27**, 1519 (1993).
- <sup>54</sup>M. Ikeda, H. Ariyoshi, J. Kambayashi, M. Sakon, T. Kawasaki, and M. Monden, *J. Cell. Biochem.* **61**, 292 (1996).
- <sup>55</sup>C. J. Jen, H. I. Chen, K. C. Lai, and S. Usami, *Blood* **87**, 3775 (1996).
- <sup>56</sup>L. M. Waples, O. E. Olorundare, S. L. Goodman, Q. J. Lai, and R. M. Albrecht, *J. Biomed. Mater. Res.* **32**, 65 (1996).
- <sup>57</sup>L. M. Waples, O. E. Olorundare, S. L. Goodman, and R. M. Albrecht, *Cells Mater.* **2**, 299 (1992).
- <sup>58</sup>H. M. van Zijp, A. D. Barendrecht, J. Riegman, J. M. Goudsmits, A. M. de Jong, H. Kress, and M. W. Prins, *Biomed. Microdevices* **16**, 217 (2014).
- <sup>59</sup>I. Reviakine, *Biointerphases* **8**, 26 (2013).
- <sup>60</sup>V. Gassing, T. Douglas, P. H. Warnke, Y. Acil, J. Wiltfang, and S. T. Becker, *Clin. Oral Implants Res.* **21**, 543 (2010).
- <sup>61</sup>V. Parazzi, L. Lazzari, and P. Rebullia, *Platelets* **21**, 549 (2010).
- <sup>62</sup>K. Bieback, *Transfus. Med. Hemother.* **40**, 326 (2013).
- <sup>63</sup>A. Mishra, P. Tummala, A. King, B. Lee, M. Kraus, V. Tse, and C. R. Jacobs, *Tissue Eng., Part C* **15**, 431 (2009).
- <sup>64</sup>A. A. Thyparambil, Y. Wei, and R. A. Latour, *Biointerphases* **10**, 019002 (2015).
- <sup>65</sup>B. Sivaraman and R. A. Latour, *Biomaterials* **31**, 1036 (2010).
- <sup>66</sup>B. Sivaraman and R. A. Latour, *Langmuir* **28**, 2745 (2012).
- <sup>67</sup>H. Shankaran, P. Alexandridis, and S. Neelamegham, *Blood* **101**, 2637 (2003).
- <sup>68</sup>C. A. Siedlecki, B. J. Lestini, K. K. Kottke-Marchant, S. J. Eppell, D. L. Wilson, and R. E. Marchant, *Blood* **88**, 2939 (1996).
- <sup>69</sup>S. W. Schneider, S. Nuschele, A. Wixforth, C. Gorzelanny, A. Alexander-Katz, R. R. Netz, and M. F. Schneider, *Proc. Natl. Acad. Sci. U.S.A.* **104**, 7899 (2007).
- <sup>70</sup>F. Kirschhofer, A. Rieder, C. Prechtel, B. Kuhl, K. Sabljo, C. Woll, U. Obst, and G. Brenner-Weiss, *Anal. Chim. Acta* **802**, 95 (2013).
- <sup>71</sup>J. Lazarovits, Y. Y. Chen, E. A. Sykes, and W. C. Chan, *Chem. Commun.* **51**, 2756 (2015).
- <sup>72</sup>M. J. Dijkstra-Tiekstra, P. F. van der Meer, R. Cardigan, D. Devine, C. Prowse, P. Sandgren, and J. de Wildt-Eggen, *Transfusion* **51**, 38S (2011).
- <sup>73</sup>P. F. van der Meer, J. A. Cancelas, R. R. Vassallo, N. Rugg, M. Einarson, and J. R. Hess, *Transfusion* **51**, 45S (2011).
- <sup>74</sup>S. Braune, M. Walter, F. Schulze, A. Lendlein, and F. Jung, *Clin. Hemorheol. Microcirc.* **58**, 159 (2014).

## Supporting Information.

# Differences in intracellular calcium dynamics cause differences in $\alpha$ -granule secretion and phosphatidyl serine expression in platelets adhering on glass and TiO<sub>2</sub>.

Swati Gupta,<sup>1,2</sup> Alessia Donati,<sup>3</sup> and Ilya Reviakine<sup>3,4\*</sup>

1 Biosurfaces, CIC biomaGUNE, Paseo Miramón 182, San Sebastián, 20009, Spain

2 Department of Biochemistry and Molecular Biology, University of the Basque Country, 28940 Leioa, Spain

3 Institute of Functional Interfaces (IFG), Karlsruhe Institute of Technology (KIT), Hermann-von Helmholtz-Platz 1, 76344 Eggenstein-Leopoldshafen, Germany

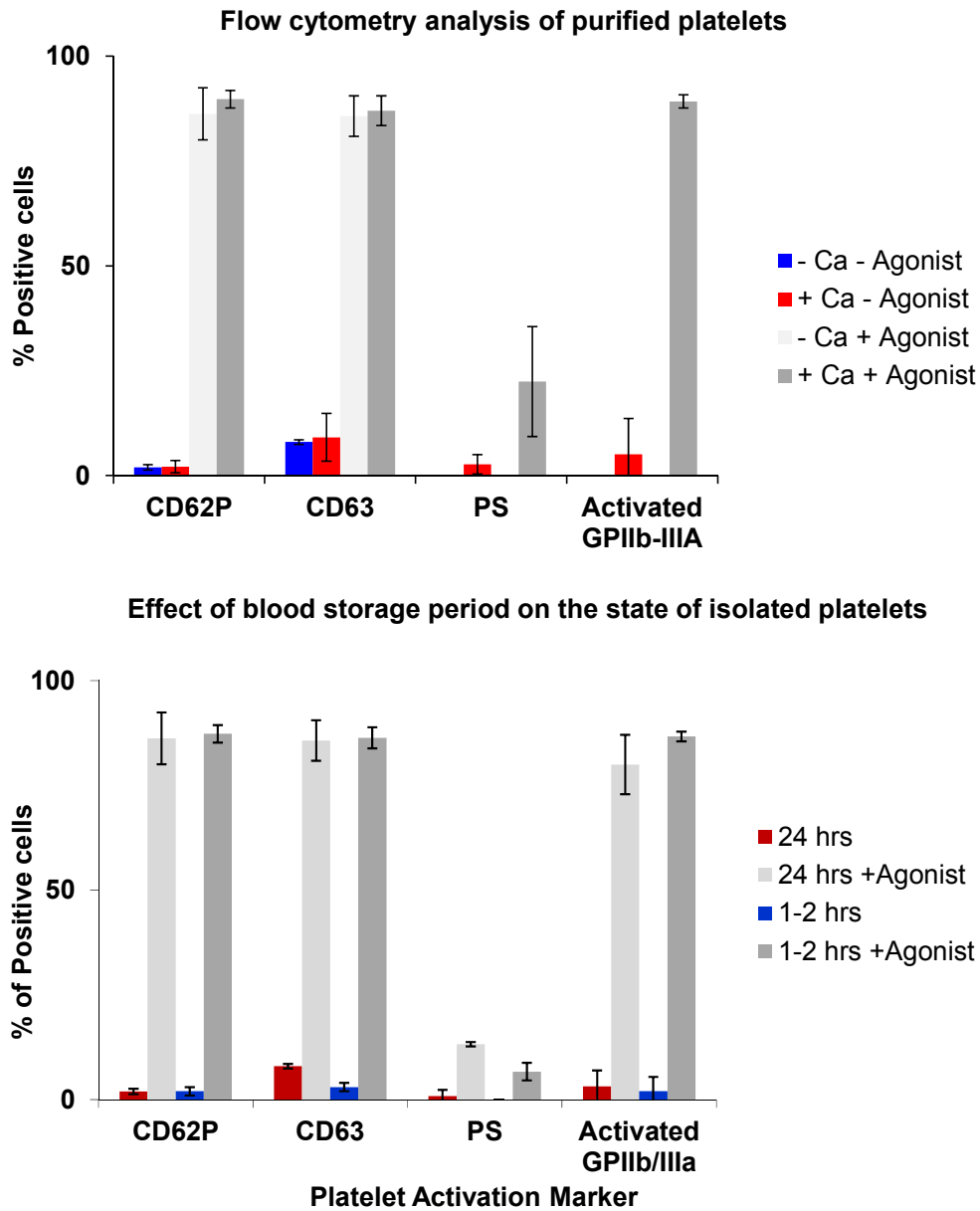
4 Department of Bioengineering, University of Washington - Seattle, USA

\* Corresponding author: Ilya.Reviakine@kit.edu

## Contents

Figure S1: Flow Cytometry characterization of purified platelets.....	3
Figure S2: Expression of CD63 does not differ on platelets adhering on glass and TiO <sub>2</sub> .....	5
Figure S3: Expression of the $\alpha$ -granule marker on freshly purified platelets adhering on TiO <sub>2</sub> ....	6
Movie S4: Intracellular Calcium Dynamics in Platelets Adhering on TiO <sub>2</sub> .....	7
Movie S5: Intracellular Calcium Dynamics in Platelets Adhering on Glass.....	7
Figure S6. Cell viability assay of platelets adhering on glass and TiO <sub>2</sub> surfaces.....	8
Figure S7: PS and GPIIb/IIIa expression in freshly purified platelets adhering on TiO <sub>2</sub> .....	9

**Figure S1: Flow Cytometry characterization of purified platelets.**



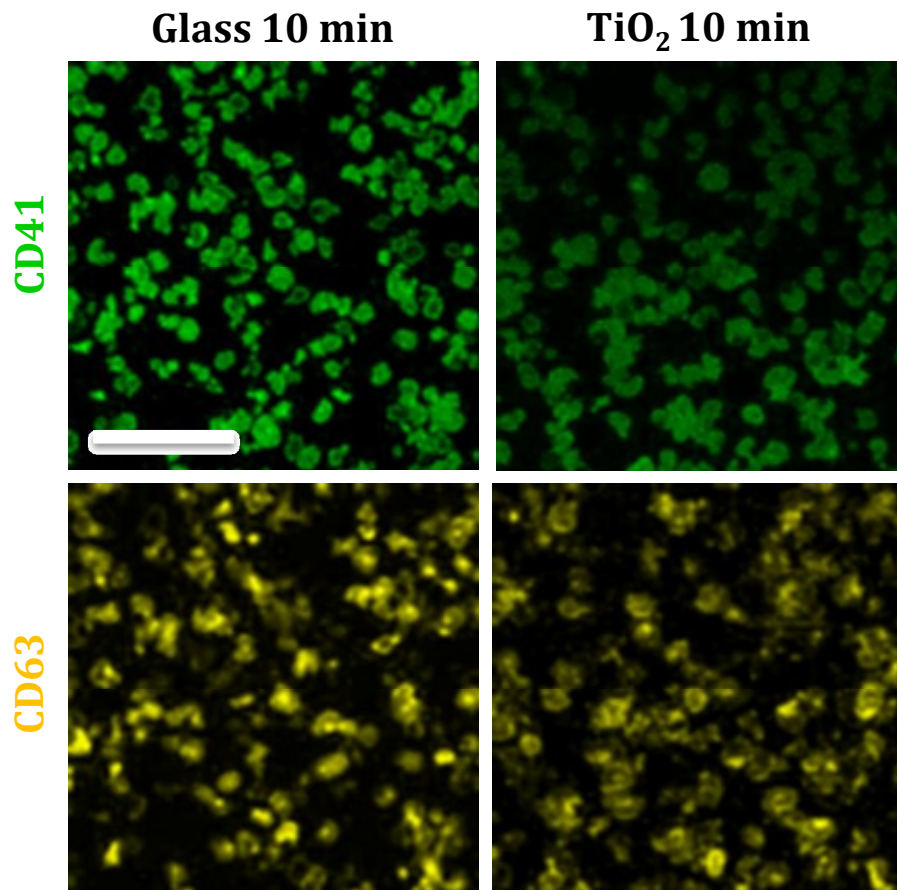
(A) Freshly isolated platelets were analyzed by flow cytometry to ascertain the level of activation marker expression (CD62P, CD63, PS and activated GPIIb/IIIa) and response to agonists (TRAP for CD62P, CD63, and PS, PMA for GPIIb/IIIa) in the presence and in the absence of calcium. It can be seen that in the absence of an agonist, activation marker expression is very

small. Agonist treatment leads to platelet activation as judged from the expression of the activation markers both in the presence and in the absence of extracellular calcium, as expected.

(B) Evaluating the effect of blood storage time on level of activation and response to agonists in freshly isolated platelets. Platelets isolated from blood that was stored for ~ 2 hrs vs. from blood that was stored for 24 hrs after extraction. In both cases, blood was stored at room temperature, and the isolation and purification protocols were the same. CD63 expression on the platelets isolated the blood stored for 24 hrs was slightly higher than that on those isolated from fresh blood. Otherwise, in terms of the activation marker expression, both sets of platelets behaved in a similar manner.

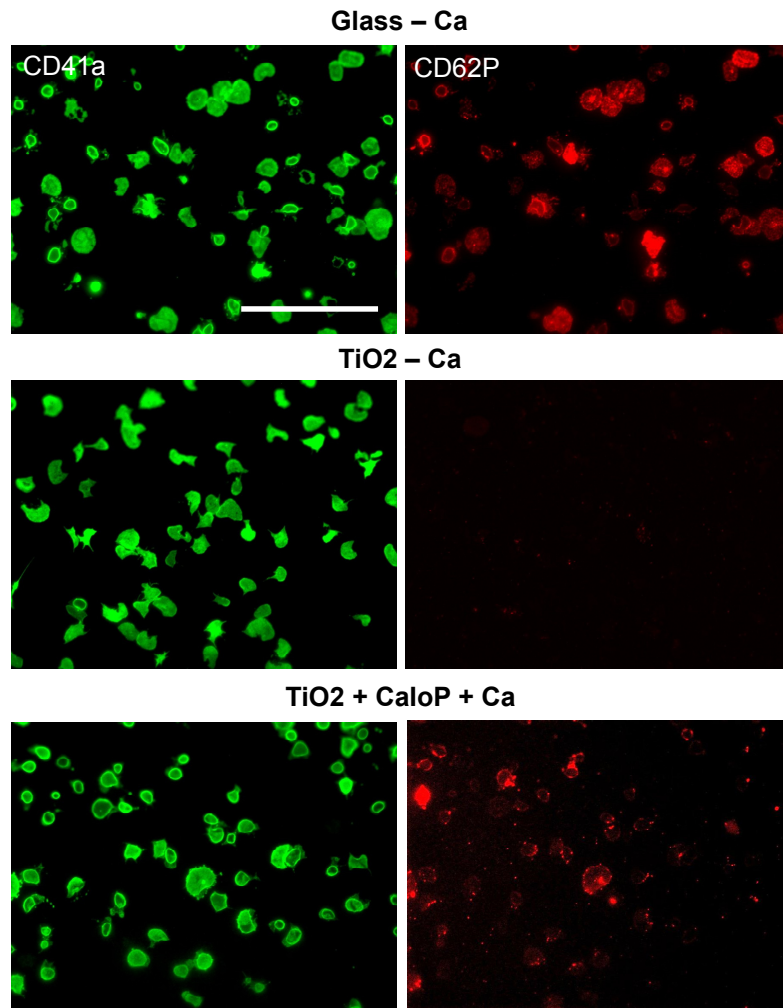
Averaged results from three independent experiments (different donors) are shown.

**Figure S2: Expression of CD63 does not differ on platelets adhering on glass and TiO<sub>2</sub>.**



Immunofluorescence staining of platelets adhering on glass (left) and TiO<sub>2</sub> (right) for 10 minutes in a calcium-free buffer for CD63 reveals similar expression patterns on both surfaces. Details can be found in our previous publication.<sup>1</sup> The scale bar is 50  $\mu$ m.

**Figure S3: Expression of the  $\alpha$ -granule marker on freshly purified platelets adhering on  $\text{TiO}_2$ .**



Platelets purified from blood within 30 min of phlebotomy were allowed to adhere on glass (top) and  $\text{TiO}_2$  (middle, bottom) for 10 minutes in the absence of extracellular calcium. The adhering platelets were washed and stained with fluorescently labeled antibodies against CD41a (green) and CD62P (red). While platelets adhering on glass express CD62P, platelets adhering on  $\text{TiO}_2$  do not (middle). Treating them with CaloP in the

presence of calcium triggers CD62P expression (bottom). Representative images from 5 independent experiments (different donors) are shown. The scale bar is 50  $\mu\text{m}$ .

**Movie S4: Intracellular Calcium Dynamics in Platelets Adhering on TiO<sub>2</sub>.**

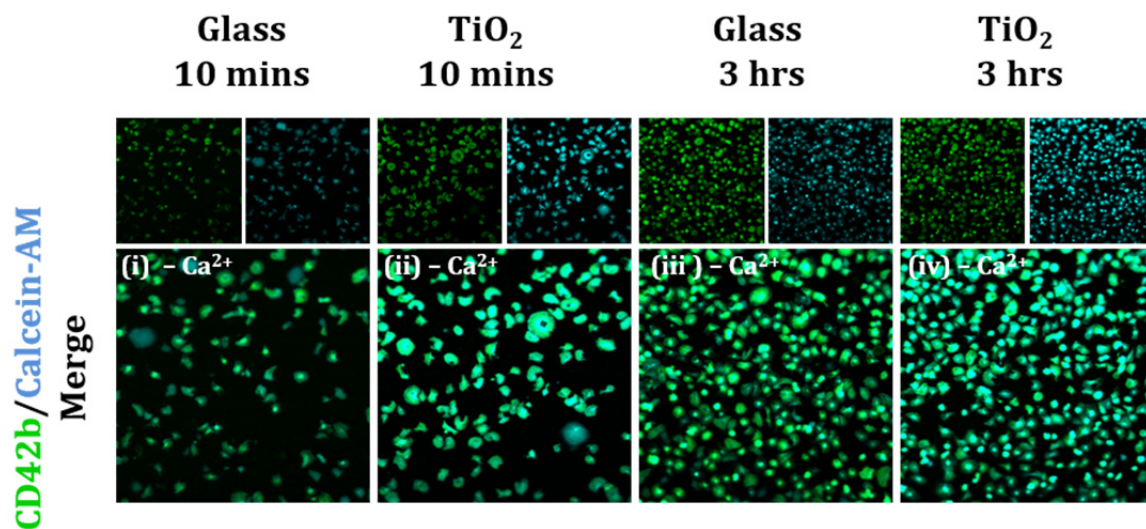
A time-lapse sequence of scanning laser confocal fluorescence microscopy images of platelets adhering on the surface of TiO<sub>2</sub>. Transmission images, merged with the calcein red orange (green) and the calcium-sensitive fluo-3 (red) dyes, are shown. The frames are  $34 \times 34 \mu\text{m}^2$ , and the entire sequence takes 292 s in real time.

**Movie S5: Intracellular Calcium Dynamics in Platelets Adhering on Glass.**

A time-lapse sequence of scanning laser confocal fluorescence microscopy images of platelets adhering on glass. Transmission images, merged with the calcein red orange (green) and the calcium-sensitive fluo-3 (red) dyes, are shown. The frames are  $34 \times 34 \mu\text{m}^2$ , and the entire sequence takes 250 s in real time.

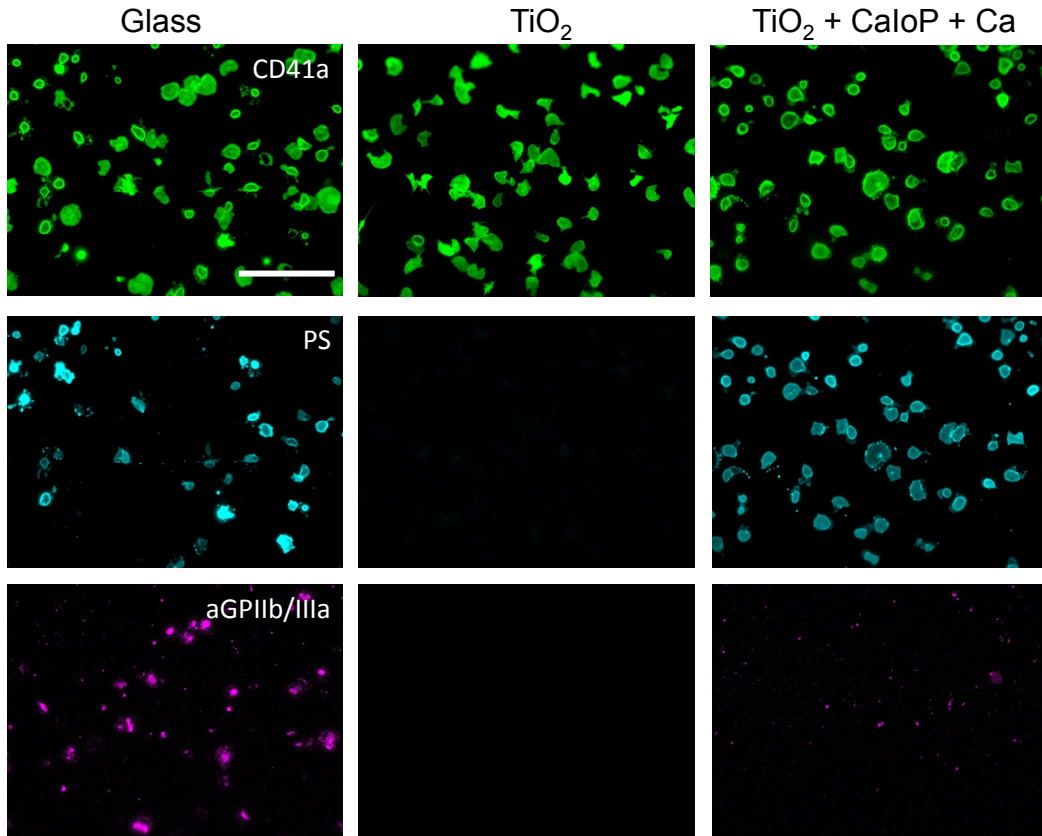
Further details of the experiments depicted in these sequences can be found in the legend of Figure 2 in the main text.

**Figure S6. Cell viability assay of platelets adhering on glass and TiO<sub>2</sub> surfaces.**



Platelets were incubated with TiO<sub>2</sub>-coated (ii and iv) or bare glass cover slips (i and iii) for 10 minutes or for 3 hours in a nominally Ca<sup>2+</sup>-free buffer and extensively washed with the same buffer. Platelets that remained on the surface were incubated with the anti-CD42b antibody (green) and an intracellular cytoplasmic dye calcein AM (blue) and observed in the confocal microscope. Cells adhered on both glass and TiO<sub>2</sub> surfaces were viable as they stained with calcein AM dye (blue and merged images), which would have leaked out if platelets were not viable or if membrane was damaged.

**Figure S7: PS and GPIIb/IIIa expression in freshly purified platelets adhering on TiO<sub>2</sub>.**



For this experiment, platelets were purified within 30 minutes after phlebotomy and allowed to adhere to freshly cleaned glass (left) and TiO<sub>2</sub> (middle, right) surfaces in the calcium-free buffer for 10 minutes. Samples were then rinsed with the same buffer, and the buffer was replaced with one containing 2 mM calcium. The samples were stained with aCD41a (green), annexin A5 (magenta) to reveal PS expression, and the antibody against the activated form of GPIIb/IIIa (PAC1, purple). CaloP was added to some of the samples prior to immunostaining (right), incubated for 30 minutes. Consistent with the images shown in Figure 3 and Figure 4 in the main text, platelets adhering on TiO<sub>2</sub> do not express PS or aGPIIb/IIIa (middle). CaloP treatment triggers PS expression but not the activation of GPIIb/IIIa. The scale bare in the top left image is 50  $\mu$ m.

**References:**

1. S. Gupta and I. Reviakine, *Biointerphases* 7, 28-40 (2012).